

# Structural and Electrical Properties of Sintered Barium-Zinc-Titanate Ceramics

N. OBRADOVIĆ<sup>a,\*</sup>, S. FILIPOVIĆ<sup>a</sup>, V. PAVLOVIĆ<sup>a</sup>, V. PAUNOVIĆ<sup>b</sup>, M. MITRIĆ<sup>c</sup> AND M.M. RISTIĆ<sup>d</sup>

<sup>a</sup>Institute Of Technical Sciences Of Sasa, Knez-Mihailova 35/Iv, 11000 Belgrade, Serbia

<sup>b</sup>Faculty For Electronics, University of Niš, 18000 Niš, Serbia

<sup>c</sup>The Vinča Institute Of Nuclear Sciences, Mike Alasa 14-16, 11000 Belgrade, Serbia

<sup>d</sup>Serbian Academy Of Sciences And Arts, Knez-Mihajlova 35, 11000 Belgrade, Serbia

The aim of this work was an investigation of structural and electrical properties of sintered barium-zinc-titanate ceramics. Mixtures of BaCO<sub>3</sub>, ZnO and TiO<sub>2</sub> were mechanically activated in a planetary ball mill up to 80 minutes and sintered isothermally in air for 120 minutes at 1300 °C. The phase composition in the BaCO<sub>3</sub>-ZnO-TiO<sub>2</sub> system after milling and sintering was analyzed using the XRD method. The existence of pure barium-zinc-titanate has been registered. Microstructure analyses were performed using SEM. The results of electric resistivity, capacitance and loss tangent of the sintered samples were correlated with the XRD and SEM results.

PACS: 81.20.Wk, 81.20.Ev, 61.05.C-, 84.37.+q

## 1. Introduction

Compounds based on barium-titanate are some of the most studied among others compounds in materials science owing to their variety of application. They attract significant attention due to their specific microwave properties. They are commonly used as parts of resonators, filters and multilayer ceramic capacitors [1]. Many investigations have been performed in order to improve successful synthesis process of BaO-TiO<sub>2</sub> various compounds, as well as their dielectric properties [2–7]. One of the desirable compounds is BaZn<sub>2</sub>Ti<sub>4</sub>O<sub>11</sub> with the ratio of the starting oxides being close to 1:2:4. There are a few intentions to obtain pure crystal phase with the mentioned structure, present in various commercial microwave dielectric materials [1, 8].

It is known that material properties depend on their synthesis process, as their physical-chemical properties are influenced by the synthesis conditions. Since low-temperature sintering is a desirable property for many microwave dielectrics, the sintering temperature can be lowered if barium-zinc-titanate is prepared in nanocrystalline form. Recently it has been established that high-energy ball milling can be used for producing nanocrystalline materials. This method has many advantages, such as simplicity, relatively inexpensive production, applicability to any class of materials, etc [9, 10].

Taking this into account, in this article, the authors have studied mechanical activation of BaCO<sub>3</sub>-ZnO-TiO<sub>2</sub> system, and its sintering, in order to obtain a pure dense barium-zinc-titanate ceramics and to reveal structural and electrical properties of sintered ceramics.

## 2. Experimental procedure

Mixtures of BaCO<sub>3</sub> (99% Sigma-Aldrich), ZnO (99% Sigma-Aldrich) and TiO<sub>2</sub> powders (99.8% Sigma-Aldrich) at a molar ratio BaCO<sub>3</sub>:ZnO:TiO<sub>2</sub> = 1 : 2 : 4 were mechanically activated by grinding in a high energy planetary ball mill device (Retsch type PH 100), with zirconium oxide balls and vessels. The milling process was performed in air for 20, 40 and 80 minutes at a basic disc rotation speed of 400 rpm. Ball to powder mixture mass ratio was 20:1. Samples were denoted as BZT-0 to BZT-80, according to the milling time.

The binder-free powders were compacted using the uniaxial double action pressing process in an 8 mm diameter tool (Hydraulic press RING, P-14, VEB THURINGER). Compacts were placed in an alumina boat and heated in a tube furnace (Lenton Thermal Design Typ 1600). The heating rate was 10 °C/min and when the temperature of the furnace reached 1300 °C, compacts were sintered isothermally in air atmosphere for 120 minutes. The density of specimens was calculated from measurements of specimen's diameter, thickness and mass.

X-ray powder diffraction patterns after milling and heating were obtained using a Philips PW-1050 diffrac-

\* corresponding author; e-mail: nina.obradovic@itn.sanu.ac.rs

tometer with  $\lambda\text{Cu-K}\alpha$  radiation and a step/time scan mode of  $0.05^\circ/1\text{s}$ .

The morphology of obtained samples was characterized by scanning electron microscopy (JEOL JSM-6390 LV). The powders were cracked and covered with gold in order to perform these measurements.

The measurements of electrical resistivity, capacitance and loss tangent of samples were measured in the frequency range from 20 Hz to 1 MHz with a LCR meter AGILENT 4284A. The samples were prepared by painting silver electrodes on both sides following with thermal treatment at  $120^\circ\text{C}$  for 2h performed in order to improve the paint conductivity.

### 3. Results and discussion

X-ray diffraction patterns of non-milled and ball-milled  $\text{BaCO}_3$ ,  $\text{ZnO}$  and  $\text{TiO}_2$  powders are given in Fig. 1.

BZT-0 is the X-ray pattern of the non-milled starting mixture containing  $\text{BaCO}_3$ ,  $\text{ZnO}$  and  $\text{TiO}_2$  (anatase and rutile modification). The identification of all obtained reflections has been accomplished using the JCPDS cards (86-1157 for  $\text{TiO}_2$  anatase, 71-2394 for  $\text{BaCO}_3$ , 89-0510 for  $\text{ZnO}$ , 76-0326 for  $\text{TiO}_2$  rutile, 75-1582 for  $\text{TiO}_2$  brookite, 87-1781 for  $\text{Zn}_2\text{Ti}_3\text{O}_8$ , 82-1175 for  $\text{BaTiO}_3$ , 85-0547 for  $\text{ZnTiO}_3$  and 81-2380 for  $\text{BaZn}_2\text{Ti}_4\text{O}_{11}$ ). No  $\text{ZrO}_2$  peaks were detected, so we assume that no powder contamination occurred during the milling process. BZT-20 diffraction pattern indicated that the process of amorphization is taking place along with peak broadening. We can also notice the appearance of  $\text{BaTiO}_3$ ,  $\text{ZnTiO}_3$  and metastable  $\text{Zn}_2\text{Ti}_3\text{O}_8$  phases and disappearance of  $\text{TiO}_2$  rutile and brookite phases.

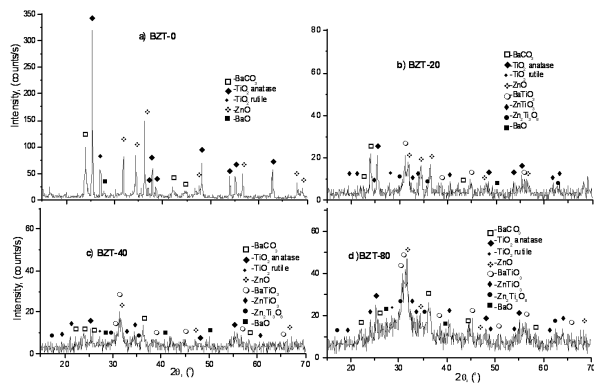


Fig. 1. XRD patterns of samples: a) BZT-0, b) BZT-20, c) BZT-40 and d) BZT-80.

As the time of activation is prolonged, the less intensities and greater broadening of all peaks are observed. In the BZT-40 pattern, we can notice the simultaneous decrease of  $\text{TiO}_2$  anatase,  $\text{ZnO}$  and  $\text{BaCO}_3$  with an increase of  $\text{BaTiO}_3$ ,  $\text{ZnTiO}_3$  and  $\text{Zn}_2\text{Ti}_3\text{O}_8$  phases. After 80 minutes of activation, all phases mentioned above within BZT-40 are still present, although the dominant

phase is a phase of  $\text{BaTiO}_3$ . Significant peak broadening, which has been observed for activated samples can be ascribed to the decrease of crystallinity that takes place in this type of powder processing and is a consequence of defect formation and diminution of crystallite size. Further prolongation of milling time would lead to formation of hard agglomerates, which are not suitable for good sinterability [11]. Analyses of microstructure parameters calculated from the XRD data, using approximation method (Sherrer's equation), indicate that the most intense changes are present in the  $\text{ZnO}$  lattice. Our previous investigation showed the decrease in crystallite size, from 112 to 31 nm for  $\text{ZnO}$ , from 80 to 35 nm for  $\text{TiO}_2$  and from 52 to 31 nm for  $\text{BaCO}_3$  and it is obvious that the crystallite size of  $\text{ZnO}$  decreases most during the milling process, for all three directions observed [12]. Taking this into account, along with changes in dislocation's density and lattice strain, one can say that the process of  $\text{ZnO}$  crystal lattice destruction is the dominant one.

Based on our previous experiments, the authors have chosen a sintering temperature of  $1300^\circ\text{C}$ , because of a fact that on lower temperatures the presence of different phases such as  $\text{BaTiO}_3$ ,  $\text{ZnTiO}_3$ ,  $\text{Ba}_4\text{ZnTi}_{11}\text{O}_{27}$  and  $\text{BaZn}_2\text{Ti}_4\text{O}_{11}$  were present. After sintering, only a pure barium-zinc-titanate phase is observed within all samples (Fig. 2). It is obvious that the reflections of the sintered samples are sharper and more intensive compared to the activated ones. This is a result of the enhanced grain growth, defect disappearance and the recrystallization that occur during sintering.

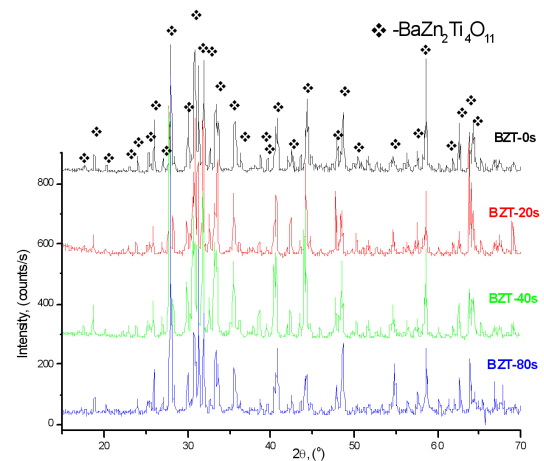


Fig. 2. XRD patterns of non activated and activated samples sintered at  $1300^\circ\text{C}$  for 2 hours.

The evolution of microstructure constituents, grains and pores which occur during the sintering process has been studied by SEM. It has been established that with temperature increase and prolonged sintering time, the adequate processes of grain growth and decrease of pore size are taking place. Microstructure analysis (Fig. 3.) showed that non-uniform grain growth is

present within BZT-0 sample along with grains greater than 20 microns. As a result of reaction sintering process the existence of large pores has been noticed as well. For the samples which have been activated for 20 min a continual matrix of closed pores, 5 microns in size was noticed. Further mechanical activation not only increased sintering densities of the samples, but also led to the increase of contact necks and strengthening of boundary regions of neighboring grains. As a result, microstructure of BZT-40 showed that the fracture occurred both between grain boundaries and through the grains, causing not so favorable microstructure. Irregularly shaped pores are present besides spherical pores as a result of BT blocks approaching. According to our analysis the most homogenous microstructure was obtained for the sample activated 80 minutes. Namely, well formed BZT phase is obtained as well as spherical and closed pores, 2 microns in size, approximately.

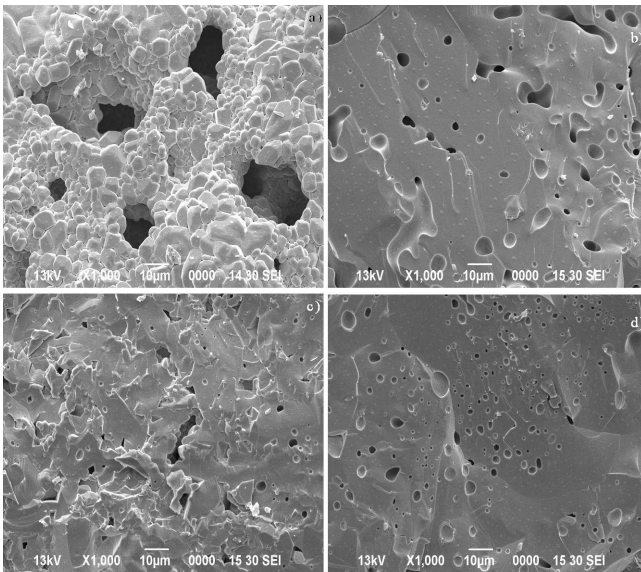


Fig. 3. SEM micrographs of samples: a) non activated, and activated for: b) 20, c) 40 and d) 80 minutes and sintered at 1300 °C for 2 hours.

The results of microstructure development are in accordance with obtained densities and dielectric properties of BZT ceramics. The values of densities obtained after sintering ( $d_S$ , given in percents of theoretical density of  $\text{BaZn}_2\text{Ti}_4\text{O}_{11}$ ), quality factor ( $Q$ ), dielectric permittivity ( $\epsilon_r$ ) and specific resistance ( $\rho$ , given in  $\Omega \text{ m}$ ) are given in Table.

The electrical measurements pointed out that dielectric permittivity of the specimens increased with activation time reaching its maximum for the sample activated 80 minutes. It is believed that the densities play an important role in controlling dielectric loss [13]. Also, it is noticed that the value of density is slightly decreased while the value of specific resistance increased for the BZT-40 sample. Having in mind greater porosity as well as the inhomogeneous structure of the mentioned sample,

we suppose that the irregular shaped pores and grains caused increase in  $\rho$  values. The  $Q$  value is generally affected not only by the lattice vibrational modes, but also by the pores, the second phases, the impurities, the lattice defect, crystallizability and inner stress [14].

TABLE

Electrical properties (at the 1 MHz frequency) and relative densities of BZT ceramics using samples: non-activated and activated for 20, 40 and 80 minutes and sintered at 1300 °C for 2 h.

sample	$d_S$ [%TD]	$\epsilon_r$	$Q$	$\tan \delta \cdot 10^{-3}$	$\rho$ [ $\Omega \text{ m}$ ]
BZT-0	70.42	41.84	92.98	10.75	4.45
BZT-20	92.37	44.61	82.61	12.11	3.87
BZT-40	91.90	51.71	56.06	17.84	6.81
BZT-80	93.12	55.22	123.09	8.12	3.11

According to our analysis, a higher density resulted in a higher dielectric permittivity owing to the lower porosity for the fixed sintering temperature. The increase in activation time is beneficial to the densification after sintering and crystallizability until the  $Q$  value reaches the maximum. The further increase in activation time will result in the appearance of abnormal grains and pores after sintering process and consequently lead to the reduction of the  $Q$  value.

This suggests that, for the activation and sintering conditions we used, a higher density and the homogeneity of morphology [15] are dominantly responsible for the higher values of dielectric permittivity of the samples.

#### 4. Conclusions

In this article the influence of mechanical activation of the  $\text{BaCO}_3\text{-ZnO-TiO}_2$  system on structural and electrical properties of sintered barium-zinc-titanate ceramics has been examined. It was noticed that the first significant appearance of barium-titanate phase along with all the starting phases is established to be after 20 minutes of mechanical treatment. The conditions of mechanical treatment led to particle size reduction, formation of different phases, but did not lead to formation of barium-zinc-titanate. A pure barium-zinc-titanate phase in all samples has been synthesized successfully after the sintering process at 1300 °C for 2h. Mechanical treatment is responsible for greater values of densities after sintering. Microstructure analyses showed that mechanical activation led to the increase of contact necks and strengthening of boundary regions of neighboring grains. Values of dielectric permittivity increased with prolonged milling time, reaching its maximum for BZT-80 ceramics ( $\epsilon_r = 55.22$ ), which makes it a good candidate for application as dielectrics.

### Acknowledgements

This research is part of Project F-7 of Serbian Academy of Sciences and Arts and Project 142011 G of Ministry for Science of the Republic of Serbia.

### References

- [1] W. Guoqing, W. Shunhua, S. Hao, *Mat. Lett.* **59**, 2229 (2005).
- [2] J.-H. Choy, Y.-S. Han, S.-H. Hwang, *J. Am. Ceram. Soc.* **81**, 3197 (1998).
- [3] K.H. Yoon, J.B. Kim, W.S. Kim, E.S. Kim, *J. Mater. Res.* **11**, 1996 (1996).
- [4] T. Negas, G. Yeager, S. Bell, N. Coats, *Am. Ceram. Soc. Bull.* **72**, 80 (1993).
- [5] W.-Y. Lin, R.F. Speyer, W.S. Hackenberger, T.R. Shrout, *J. Am. Ceram. Soc.* **82**, 1207 (1999).
- [6] X. Wang, M. Gu, B. Yang, S. Zhu, W. CaO, *Microelectron. Eng.* **66**, 855 (2003).
- [7] B.D. Stojanovic, A.Z. Simoes, C.O. Paiva-Santos, C. Jovalekic, V.V. Mitic, J.A. Varela, *J. Eur. Ceram. Soc.* **25**, 1985 (2005).
- [8] A. Balous, O. Ovchar, M. Macek-Krzmanc, M. Valant, *J. Eur. Ceram. Soc.* **26**, 3733 (2006).
- [9] O. Yamaguchi, M. Morimi, H. Kawabata, K. Shimizu, *J. Am. Ceram. Soc.* **70**, 97 (1987).
- [10] K.T. Paul, S.K. Satpathy, I. Manna, K.K. Chakraborty, G.B. Nando, *Nanoscale Res. Lett.* **2**, 397 (2007).
- [11] T. Sreckovic, N. Labus, N. Obradovic, Lj. Zivkovic, *Mat. Sci. Forum* **453-454**, 435 (2004).
- [12] N. Obradović, S. Filipović, V. Pavlović, M. Mitrić, S. Marković, V. Mitić, N. Đorđević, M.M. Ristić, *Ceram. Int.* **37**, 21 (2011).
- [13] J. Zhu, E.R. Kipkoech, W. Lu, *J. Eur. Ceram. Soc.* **26**, 2027 (2006).
- [14] W. Lei, J.H. Zhu, X.H. Wang, *Mater. Lett.* **61**, 4066 (2007).
- [15] X. Liu, F. Gao, C. Tian, *Mater Res. Bull.* **43**, 693 (2008).